Journal of Computational Physics 385 (2019) 13–32

Contents lists available at ScienceDirect

Journal of Computational Physics

www.elsevier.com/locate/jcp

Numerical methods for porous medium equation by an energetic variational approach

Chenghua Duan [a,b], Chun Liu [c], Cheng Wang [d], Xingye Yue [b,*]

[a] Shanghai Center for Mathematical Sciences, Fudan University, Shanghai 200438, China
[b] Department of Mathematics, Soochow University, Suzhou 215006, China
[c] Department of Applied Mathematics, Illinois Institute of Technology, Chicago, IL 60616, USA
[d] Department of Mathematics, University of Massachusetts, Dartmouth, North Dartmouth, MA, 02747-2300, USA

ARTICLE INFO

Article history:
Received 27 June 2018
Received in revised form 27 January 2019
Accepted 28 January 2019
Available online 22 February 2019

Keywords:
Energetic variational approach
Porous medium equation
Finite speed propagation of free boundary
Waiting time
Trajectory equation

ABSTRACT

We study numerical methods for porous media equation (PME). There are two important characteristics: the finite speed propagation of the free boundary and the potential waiting time, which make the problem difficult to handle. Based on different dissipative energy laws, we develop two numerical schemes by an energetic variational approach. Firstly, based on $f \log f$ as the total energy form of the dissipative law, we obtain the trajectory equation, and then construct a fully discrete scheme. It is proved that the scheme is uniquely solvable on an admissible convex set by taking the advantage of the singularity of the total energy. Next, based on $1/(2f)$ as the total energy form of the dissipation law, we construct a linear numerical scheme for the corresponding trajectory equation. Both schemes preserve the corresponding discrete dissipation law. Meanwhile, under some smoothness assumption, both schemes are second-order convergent in space and first-order convergent in time. Each scheme yields a good approximation for the solution and the free boundary. No oscillation is observed for the numerical solution around the free boundary. Furthermore, the waiting time problem could be naturally treated, which has been a well-known difficult issue for all the existing methods. Due to its linear nature, the second scheme is more efficient.

1. Introduction and background

The porous medium equation (PME) can be found in many physical and biological phenomena, such as the flow of an isentropic gas through a porous medium [27], the viscous gravity currents [20], nonlinear heat transfer and image processing; e.g., see [44]. The aim of this paper is to provide numerical methods for the PME

$$\partial_t f = \Delta_x(f^m),\ x \in \Omega \subset \mathbb{R}^d,\ m > 1,$$

where $f := f(x,t)$ is a non-negative scalar function of space $x \in \mathbb{R}^d$ $(d \geq 1)$ and the time $t \in \mathbb{R}^+$, and m is a constant larger than 1.

The PME is a nonlinear degenerate parabolic equation since the diffusivity $D(f) = mf^{m-1} = 0$ at points where $f = 0$. In turn, the PME has a special feature: the finite speed of propagation [44]. If the initial data has a compact support, the

* Corresponding author.
E-mail addresses: chduan@fudan.edu.cn (C. Duan), cliu124@iit.edu (C. Liu), cwang1@umassd.edu (C. Wang), xyyue@suda.edu.cn (X. Yue).

https://doi.org/10.1016/j.jcp.2019.01.055
0021-9991/

solution of Cauchy problem of the PME will have a compact support at any given time $t > 0$. The interface between the compact support and zero-value region is called as free boundary. In comparison with a heat equation, which can smooth out the initial data, the solution of the PME could become non-smooth even if the initial data is smooth with compact support. Moreover, for certain initial data, the solution of the PME can exhibit a waiting time phenomenon where the free boundary remains stationary until a finite positive time (called *waiting time*). After that time instant, the interface begins to move with a finite speed.

Many theoretical analyses have been derived in the existing literature, including the earlier works by Oleĭnik et al. [35], Kalašnikov [25], Aronson [1], the recent work by Shmarev [40,41] and the monograph by Vázquez [44], etc. Among them, a fundamental example of solution is the Barenblatt solution [3,38,48], which has the explicit formula and a compact support at any time $t > 0$.

Various numerical methods have been studied for the PME. Graveleau & Jamet [19] and DiBenedetto & Hoff [12] solved the pressure PME equation, using the finite difference approach and tracking algorithm (containing a numerical viscosity term), respectively. Jin et al. [24] established the relaxation scheme which reformulates the PME as a linear hyperbolic system with stiff relaxation term. However, most existing numerical solutions may contain oscillations near the free boundary, such as PCSFE method (Predictor-Correction Algorithm and Standard Finite element method) [49]. In recent years, a local discontinuous Galerkin finite element method by Zhang & Wu [49] and Variational Particle Scheme (VPS) by Westdickenberg & Wilkening [47] have been used to solve the PME. These two methods can effectively eliminate non-physical oscillation in the computed solution near the free boundary, which in turn lead to a high-order convergence rate within the smooth part of the solution support. However, no relevant theoretical justification of the convergence analysis is available for these works. More recently, Huang & Ngo [34] studied an adaptive moving mesh finite element method to solve the PME with three types of metric tensor: uniform, arclength-based and Hessian-based adaptive meshes. The numerical results indicate that a first-order convergence for uniform and arclength-based adaptive meshes, and a second-order convergence for the Hessian-based adaptive mesh, while minor oscillations are observed around the free boundary in the computed solutions. Again, no theoretical proof has been available for the convergence rate in these works. A similar work to our approach could be found in [5,6], which is based on the diffeomorphism. For the initial state with a compact support, the authors solve a regularized equation. However, it may change the physical property of the original system. For example, the waiting time phenomenon can not be simulated effectively by this method.

There have also been some numerical works for the waiting time phenomenon. For example, Mimura et al. [31], Bertsch & Dal Passo [4] and Tomoeda & Mimura [43] estimated the waiting time by a postprocess. However, the numerical interface actually has a velocity from the beginning in their approaches, which may yield an inaccurate solution. Nakaki & Tomoeda [32] transformed the PME into another problem whose solution will blow up at a finite time, which is just the waiting time of PME, while the solution cannot be obtained after the waiting time.

In this paper, we construct numerical methods for PME by an Energetic Variational Approach (EnVarA) to naturally keep the physical laws, such as the conservation of mass, energy dissipation and force balance. Meanwhile, based on different dissipative energy laws, we can construct different numerical schemes. We start from the energy dissipation law:

$$\frac{d}{dt}\int_{\Omega}\omega(f)dx = -\int_{\Omega}\eta(f)|\mathbf{u}|^2dx, \tag{1.1}$$

where $\omega(f)$ is the free energy density, $\eta(f)$ is a functional of f determined by $\omega(f)$ and $\mathbf{u}$ is the velocity. The quantity $\omega(f)$ and $\eta(f)$ can be taken as follows:

- Case 0. $\omega(f) = \dfrac{1}{m-1}f^m$, and $\eta(f) = f$.
- Case 1. $\omega(f) = f\ln f$, and $\eta(f) = \dfrac{f}{mf^{m-1}}$.
- Case 2. $\omega(f) = \dfrac{1}{2f}$, and $\eta(f) = \dfrac{1}{mf^m}$.

Based on these energy dissipation laws, different numerical schemes of the trajectory equation can be derived. The numerical scheme based on the energy law in Case 0 has been studied by Westdickenberg & Wilkening [47], called as a Variational Particle Scheme (VPS).

We focus on the numerical methods based on the energy laws in the next two cases. Note that, with a vanishing f, the energy in the first case is regular while the energy in the next two cases is singular. Taking the advantage of the singularity, we can prove that the numerical schemes based on last two energy forms have some good properties such as conservation of positivity, unique solvability on an admissible convex set, convergence of the corresponding Newton's iteration.

Theoretically, the discrete energy dissipation law is proved to be valid. In addition, by a higher order expansion technique [15,45], an optimal error estimates are presented under the assumption of smooth solutions. For Cases 1 and 2, no numerical oscillation is observed near the free boundary in the extensive experiments, and the finite propagation speed of the free boundary can be effectively computed. A predictable criterion for computing waiting time is proposed and the numerical

convergence to the exact waiting time is reported, which is the first such result for the PME. In the practical computations, the numerical scheme of the trajectory equation in Case 2 is linear and hence more efficient.

This paper is organized as follows. The EnVarA and the trajectory equation of the PME are outlined in Section 2. The numerical scheme is described in Section 3. Subsequently, the proof of unique solvability, energy stability and optimal rate convergence analysis is provided in Section 4. Finally, the numerical results are presented in Section 5, including examples with positive initial state, Barenblatt Solution, a waiting time phenomenon, an initial data with two columns.

2. Trajectory equation of the PME

In this section, we derive the trajectory equation of the following initial-boundary problem of PME:

$$\partial_t f = \Delta_x(f^m),\ x \in \Omega \subset \mathbb{R}^d,\ m > 1,\ t > 0, \tag{2.1}$$

$$f(x,0) = f_0(x) \geq 0,\ x \in \Omega, \tag{2.2}$$

$$\nabla_x f \cdot \mathbf{n} = 0,\ x \in \partial\Omega,\ t > 0, \tag{2.3}$$

where f is a non-negative function, Ω is a bounded domain and $\mathbf{n}$ is the external normal direction.

2.1. The energetic variational approach

An Energetic Variational Approach (EnVarA) leads to the trajectory equation (also called *constitution relation*) based on a balance between the maximal dissipation principle (MDP) and the least action principle (LAP). The approach was originated from Onsager's pioneering work [36,37] and improved by J.W. Strutt (Lord Rayleigh) [42]. In recent years, it has been applied to model some complex systems, for example Liu & Wu [29], Hyon et al. [22], Du et al. [13], Eisenberg et al. [16] and Koba et al. [26]. Its application to the Wright-Fisher model has been studied in [14]. The detailed structures of EnVarA can be found in [14,22,29,30].

(A) Mass conservation.

In the Eulerian coordinate, the mass conservation law is

$$\partial_t f + \nabla \cdot (f\mathbf{u}) = 0, \tag{2.4}$$

where f is the density and $\mathbf{u}$ is the velocity.

In the Lagrangian coordinate, its solution can be expressed by:

$$f(x(X,t),t) = \frac{f_0(X)}{\det \frac{\partial x(X,t)}{\partial X}}, \tag{2.5}$$

where $f_0(X)$ is the positive initial data and $\det \frac{\partial x(X,t)}{\partial X}$ is the determinant of *deformation gradient*.

(B) Energy Dissipation Law (EDL) Step.

The basic energy dissipation law of PME we are going to consider is

$$\frac{d}{dt}\int_\Omega \omega(f)dx = -\int_\Omega \eta(f)|\mathbf{u}|^2 dx, \tag{2.6}$$

where the total energy $E^{total} := \int_\Omega \omega(f)dx$ with the free energy density $\omega(f)$, and $\Delta := \int_\Omega \eta(f)|\mathbf{u}|^2 dx$ is the dissipation term with the velocity $\mathbf{u}$.

(C) Least Action Principle (LAP) Step.

LAP states that the trajectories of particles from the position $x(X,0)$ at time $t = 0$ to $x(X,T^*)$ at a given time T^* in Hamiltonian system are those which minimize the action functional defined by

$$\mathcal{A}(x) := -\int_0^{T^*} \mathcal{F}dt = -\int_0^{T^*}\int_\Omega \omega\left(\frac{f_0(X)}{\det \frac{\partial x}{\partial X}}\right)\det\frac{\partial x}{\partial X}dXdt,$$

where $\mathcal{F}$ is the Helmholtz free energy.

Taking the variational of $\mathcal{A}(x)$ with respect to x, we have the conservation force in Eulerian coordinate, i.e.,

$$F_{con} := \frac{\delta \mathcal{A}}{\delta x} = -\nabla(f\omega'(f) - \omega) = -f\nabla\omega'(f),$$

where δ refers to the variational of the respective quantity.

(D) Maximum Dissipation Principle (MDP) Step.

MDP, i.e., Onsager's Principle, can be done by taking the variational of $\frac{1}{2}\Delta$ with respect to the velocity $\mathbf{u}$. In turn, we can obtain the dissipation force,

$$F_{dis} := \frac{\delta \frac{1}{2}\Delta}{\delta \mathbf{u}} = \eta(f)\mathbf{u}.$$

The factor $\frac{1}{2}$ is needed since that the energy dissipation Δ is always a quadratic function of certain rates such as the velocity within the linear response theory [42].

(E) Force Balance Law Step.

Based on the Newton's force balance law:

$$F_{con} = F_{dis},$$

we have the constitution relation:

$$f\nabla\omega'(f) = -\eta(f)\mathbf{u},$$

which is just

$$\frac{f^2\omega''(f)\nabla f}{\eta(f)} = -f\mathbf{u}. \tag{2.7}$$

Comparing PME (2.1) with (2.4), we choose $-f\mathbf{u} = \nabla(f^m)$, then

$$\frac{f^2\omega''(f)}{\eta(f)} = mf^{m-1}.$$

That means if the free energy $\omega(f)$ is given, then $\eta(f)$ will be determined. Theoretically, there are infinite kinds of energy dissipation laws of PME. We consider three of them:

- Case 0. If $\omega(f) = \frac{1}{m-1}f^m$, then $\eta(f) = f$ and the constitution relation becomes

  $$\nabla_x f^m = -f\mathbf{u}.$$

  Let $P := \frac{m}{m-1}f^{m-1}$ be the pressure. The relation is the Darcy's Law [44], i.e., $\mathbf{u} = \nabla P$.
- Case 1. If $\omega(f) = f\ln f$, then $\eta(f) = \frac{f}{mf^{m-1}}$ and the constitution relation in another form becomes

  $$\nabla_x f = -\frac{f}{mf^{m-1}}\mathbf{u}.$$

- Case 2. If $\omega(f) = \frac{1}{2f}$, then $\eta(f) = \frac{1}{mf^m}$ and the constitution relation in the third form is

  $$\nabla_x\left(\frac{1}{f}\right) = \frac{\mathbf{u}}{mf^m}.$$

  The free energy density $\frac{1}{2f}$ can lead to a linear numerical scheme for the trajectory equation.

Remark 2.1. The physical background of each energy formation is given by:

- The free energy density $w(f) = \frac{1}{m-1}f^m$ is derived from Darcy's Law [44].
- The porous medium equation owes its name to describe the flow of an ideal gas in a homogeneous porous medium. One can consider the free energy density $w(f) = f\ln f$ as the entropy of ideal gas, and $\eta(f) = \frac{f}{mf^{m-1}}$ contains all the information of the viscosity of the fluid and the permeability of the medium.
- $\frac{1}{2f}$ can be considered as the free energy density for the inhomogeneous linear elasticity in non-homogeneous media [7]. Other information as the entropy production is included in $\eta(f) = \frac{1}{mf^m}$.

In fact, all the trajectory equations are equivalent. However, corresponding numerical discretization leads to different schemes associated with different energy laws.

2.2. Trajectory equation of PME in 1-Dim

Combining with (2.5), we can write the constitution relation in the Lagrangian coordinate system, called as the trajectory equation. In this paper, we consider one dimensional problems. Replacing $\mathbf{u}$ with $x_t(X,t)$, we have the trajectory equation as

- Case 0.

$$f_0(X)\partial_t x = -\partial_X\left[\left(\frac{f_0(X)}{\partial_X x}\right)^m\right],\quad X\in\Omega, \tag{2.8}$$

and the corresponding energy law in Lagrangian coordinate is

$$\frac{d}{dt}\int_\Omega \frac{1}{m-1}\left(\frac{f_0(X)}{\partial_X x}\right)^m \frac{\partial x}{\partial X}dX = -\int_\Omega f_0(X)|x_t|^2 dX.$$

- Case 1.

$$\frac{f_0(X)}{m\left(\frac{f_0(X)}{\partial_X x}\right)^{m-1}}\partial_t x = -\partial_X\left(\frac{f_0(X)}{\partial_X x}\right),\quad X\in\Omega, \tag{2.9}$$

and the corresponding energy law in Lagrangian coordinate is

$$\frac{d}{dt}\int_\Omega f_0(X)\ln\left(\frac{f_0(X)}{\partial_X x}\right)dX = -\int_\Omega \frac{f_0(X)}{m\left(\frac{f_0(X)}{\partial_X x}\right)^{m-1}}|\partial_t x|^2 dX. \tag{2.10}$$

- Case 2.

$$\frac{(\partial_X x)^{m+1}}{m f_0(X)^m}\partial_t x = \partial_X\left(\frac{\partial_X x}{f_0(X)}\right),\quad X\in\Omega, \tag{2.11}$$

and the corresponding energy law in Lagrangian coordinate is

$$\frac{d}{dt}\frac{1}{2}\int_\Omega \frac{1}{f_0(X)}|\partial_X x|^2 dX = -\int_\Omega \frac{\partial_X x}{m\left(\frac{f_0(X)}{\partial_X x}\right)^m}|x_t|^2 dX. \tag{2.12}$$

Equations (2.8), (2.9) and (2.11) are the same thing, wrote in different forms with different energy laws. Solving them with proper initial and boundary conditions, we get the trajectory $x(X,t)$, which contains all the physics involved in the model. Substituting $x(X,t)$ into (2.5), we obtain the solution $f(x,t)$ to (2.1)-(2.3).

The initial and boundary conditions for equations (2.8), (2.9) or (2.11) should be

$$x|_{\partial\Omega} = X|_{\partial\Omega},\ t>0. \tag{2.13}$$

$$x(X,0) = X,\ X\in\Omega. \tag{2.14}$$

3. Numerical method of trajectory equation

In this section, we propose some semi-implicit numerical schemes for the trajectory equations.

3.1. Semi-discrete schemes in time

Let $\tau = \frac{T}{N}$, where $N\in\mathbb{N}^+$ and T is the final time. The grid point $t_n = n\tau$, $n=0,\cdots,N$. For the temporal discretization of the trajectory equation, we have that Given x^n, find x^{n+1} such that

- Case 0.

$$f_0(X)\frac{x^{n+1}-x^n}{\tau} = -\partial_X\left[\left(\frac{f_0(X)}{\partial_X x^{n+1}}\right)^m\right],\ n=0,\cdots,N-1. \tag{3.1}$$

- Case 1.

$$\frac{f_0(X)}{m\left(\frac{f_0(X)}{\partial_X x^n}\right)^{m-1}}\frac{x^{n+1}-x^n}{\tau} = -\partial_X\left(\frac{f_0(X)}{\partial_X x^{n+1}}\right),\ n=0,\cdots,N-1. \tag{3.2}$$

- Case 2.

$$\frac{(\partial_X x^n)^{m+1}}{m f_0(X)^m}\frac{x^{n+1}-x^n}{\tau} = \partial_X\Big(\frac{\partial_X x^{n+1}}{f_0(X)}\Big),\ n=0,\cdots,N-1. \tag{3.3}$$

In summary, the trajectory equation can be written in gradient flow as

$$\gamma(x)x_t = -\frac{\delta \mathcal{W}}{\delta x}, \tag{3.4}$$

where $\gamma(x)$ is a positive function depending on space x and $\mathcal{W}$ is a functional of x. Therefore, the discrete scheme in time is given by

$$\gamma(x^n)\frac{x^{n+1}-x^n}{\tau} = -\frac{\delta \mathcal{W}(x^{n+1})}{\delta x^{n+1}},\ n=0,\cdots,N-1. \tag{3.5}$$

Assume the exact solution x^n is smooth at time t^n to make $\frac{\partial x}{\partial X}$ well-defined, $n=0,\cdots,N$, then the solution x^{n+1} to scheme (3.5) is the minimizer of the following cost functional:

$$\min_{x^{n+1}\in\Omega}\left\{\int_\Omega \gamma(x^n)\frac{|x^{n+1}-x^n|^2}{2\tau} + \mathcal{W}(x^{n+1})dX\right\}, \tag{3.6}$$

where

- Case 0

$$\gamma(x^n)=1,\ \mathcal{W}(x^{n+1}) = \frac{1}{m-1}\Big(\frac{f_0(X)}{\partial_X x}\Big)^m\frac{\partial x}{\partial X},$$

  where $f_0(X)$ is the initial function. It means that the trajectory equation can be regarded as an energy gradient flow, which has been studied by Westdickenberg and Wilkening [47]. In this paper, we focus on the following two cases:
- Case 1

$$\gamma(x^n) = \frac{f_0(X)}{m\big(\frac{f_0(X)}{\partial_X x^n}\big)^{m-1}},\ \mathcal{W}(x^{n+1}) = f_0(X)\ln\Big(\frac{f_0(X)}{\partial_X x^{n+1}}\Big).$$

- Case 2

$$\gamma(x^n) = \frac{(\partial_X x^n)^{m+1}}{m f_0(X)^m},\ \mathcal{W}(x^{n+1}) = \frac{1}{2}\frac{1}{f_0(X)}|\partial_X x^{n+1}|^2.$$

Remark 3.1. The time-discrete scheme (3.5) follows the convexity analysis for the gradient flows, originated by D. Eyre's pioneering work [17]. This idea has been successfully applied to various gradient models, such as phase field crystal [23,46], Cahn-Hilliard and its coupling with fluid motion [9–11,21], epitaxial thin film growth [8,39,28], etc. The unique solvability and energy stability analysis could be established with the help of variational inequality and energy estimate. In this article, we notice that the term associated with $\mathcal{W}(x)$ is implicitly updated due to its convexity; similar analysis could also be found in a more recent work [14] to deal with Wright-Fisher model.

3.2. The fully discrete scheme with a positive initial state

Let X_0 be the left point of Ω and $h=\frac{|\Omega|}{M}$ be the spatial step, $M\in\mathbb{N}^+$. Denote by $X_r = X(r) = X_0 + rh$, where r takes on integer or half integer values. Let $\mathcal{E}_M$ and $\mathcal{C}_M$ be the spaces of functions whose domains are $\{X_i \mid i=0,...,M\}$ and $\{X_{i-\frac{1}{2}} \mid i=1,...,M\}$, respectively. In component form, these functions are identified via $l_i = l(X_i)$, $i=0,...,M$, for $l\in\mathcal{E}_M$, and $\phi_{i-\frac{1}{2}} = \phi(X_{i-\frac{1}{2}})$, $i=1,...,M$, for $\phi\in\mathcal{C}_M$.

The difference operator $D_h:\mathcal{E}_M\to\mathcal{C}_M$, $d_h:\mathcal{C}_M\to\mathcal{E}_M$, and $\widetilde{D}_h:\mathcal{E}_M\to\mathcal{E}_M$ can be defined as:

$$(D_h l)_{i-\frac{1}{2}} = (l_i - l_{i-1})/h,\ i=1,...,M, \tag{3.7}$$

$$(d_h\phi)_i = (\phi_{i+\frac{1}{2}} - \phi_{i-\frac{1}{2}})/h,\ i=1,...,M-1, \tag{3.8}$$

$$(\widetilde{D}_h l)_i = \begin{cases} (l_{i+1}-l_{i-1})/2h, & i=1,...,M-1,\\ (4l_{i+1}-l_{i+2}-3l_i)/2h, & i=0,\\ (l_{i-2}-4l_{i-1}+3l_i)/2h, & i=M. \end{cases} \tag{3.9}$$

Denote by the admissible set

$$\mathcal{Q} := \{l \in \mathcal{E}_M \mid l_{i-1} < l_i,\ 1 \le i \le M;\ l_0 = X_0,\ l_M = X_M\}, \tag{3.10}$$

in which the particles are arranged in the order without twisting or exchanging. Its boundary set is $\partial\mathcal{Q} := \{l \in \mathcal{E}_M \mid l_{i-1} \le l_i,\ 1 \le i \le M,\ \text{and } l_i = l_{i-1},\ \text{for some } 1 \le i \le M;\ l_0 = X_0,\ l_M = X_M\}$. Then $\bar{\mathcal{Q}} := \mathcal{Q} \cup \partial\mathcal{Q}$ is a closed convex set.

The **fully discrete scheme** is formulated as follows. Given the positive initial state $f_0(X) \in \mathcal{E}_M$ and the particle position $x^n \in \mathcal{Q}$, find $x^{n+1} = (x_0^{n+1}, ..., x_M^{n+1}) \in \mathcal{Q}$ such that

- Case 1.

$$\frac{f_0(X_i)}{m\left(\frac{f_0(X)}{D_h x^n}\right)_i^{m-1}} \cdot \frac{x_i^{n+1} - x_i^n}{\tau} = -d_h\left(\frac{f_0(X)}{D_h x^{n+1}}\right)_i,\ 1 \le i \le M-1, \tag{3.11}$$

with $x_0^{n+1} = X_0$ and $x_M^{n+1} = X_M,\ n = 0, \ldots, N-1$.

To solve the nonlinear equation (3.11), we use damped Newton's iteration [33]. The key idea is to adjust the marching size to prevent the solution at next iteration escaping from the admissible set $\mathcal{Q}$.

Damped Newton's iteration. Set $x^{n+1,0} = x^n$. For $k = 0, 1, 2, \cdots$, update $x^{n+1,k+1} = x^{n+1,k} + \omega(\lambda)\delta_x$ such that

$$\begin{aligned}
&\frac{f_0(X_i)}{m\left(\frac{f_0(X)}{D_h x^n}\right)_i^{m-1}} \frac{\delta_{x_i}}{\tau} - d_h\left(\frac{f_0(X)}{(D_h x^{n+1,k})^2} D_h \delta_x\right)_i \\
&= -\frac{f_0(X_i)}{m\left(\frac{f_0(X)}{D_h x^n}\right)_i^{m-1}} \frac{x_i^{n+1,k} - x_i^n}{\tau} - d_h\left(\frac{f_0(X)}{D_h x^{n+1,k}}\right)_i,\quad 1 \le i \le M-1,
\end{aligned} \tag{3.12}$$

with $\delta_{x_0} = \delta_{x_M} = 0$,

and

$$\omega(\lambda) = \begin{cases} \frac{1}{\lambda}, & \lambda > \lambda', \\ \frac{1-\lambda}{\lambda(3-\lambda)}, & \lambda' \ge \lambda \ge \lambda^*, \\ 1, & \lambda < \lambda^*, \end{cases} \tag{3.13}$$

where $\lambda^* = 2 - 3^{\frac{1}{2}}$, $\lambda' \in [\lambda^*, 1)$ and

$$\lambda^2 := \lambda^2(J, x^{n+1,k}) = \frac{1}{a}[J'(x^{n+1,k})]^T [J''(x^{n+1,k})]^{-1} J'(x^{n+1,k}), \tag{3.14}$$

where $a := h \min\limits_{0<i<M}\{f_0(X_i)\}$, J is the corresponding energy function defined latter in (4.5), and J', J'' are the gradient vector and Hessian matrix.

- Case 2.

$$\frac{(\widetilde{D}_h x^n)_i^{m+1}}{m f_0(X_i)^m} \cdot \frac{x_i^{n+1} - x_i^n}{\tau} = d_h\left(\frac{D_h x^{n+1}}{f_0(X)}\right)_i,\ 1 \le i \le M-1, \tag{3.15}$$

with $x_0^{n+1} = X_0$ and $x_M^{n+1} = X_M,\ n = 0, \cdots, N-1$.

Note that (3.15) is a linear scheme.

After solving (3.11) in Case 1 ((3.15) in Case 2), we finally obtain the numerical solution $f_i^n := f(x^n, t^n)$ by discretizing (2.5) as

$$f_i^n = \frac{f_0(X_i)}{\widetilde{D}_h x_i^n},\ 0 \le i \le M. \tag{3.16}$$

Remark 3.2. In Section 4, it will be shown that the scheme (3.11) is equivalent to a minimization problem of a convex function over the open bounded convex admissible set $\mathcal{Q}$ in (3.10). A standard Newton's iteration may not work since it is not guaranteed that each iteration is admissible.

3.3. The discrete scheme for problems with free boundaries

Next we consider the situation of the initial data with a compact support in Ω. Due to the degeneration of the PME, the left and right interfaces appear and are defined respectively as:

$$\xi_1^t := \inf\{x \in \Omega : f(x,t) > 0, t \geq 0\},$$
$$\xi_2^t := \sup\{x \in \Omega : f(x,t) > 0, t \geq 0\}.$$

Let $\Gamma^t := [\xi_1^t, \xi_2^t] \subset \Omega$. For this kind of problems, all the trajectories start from the initial support $\Gamma^0 \subsetneqq \Omega$. We shall solve a initial-boundary value problem as:

- Case 1.

$$\frac{f_0(X)}{m\left(\frac{f_0(X)}{\partial_X x}\right)^{m-1}}\partial_t x = -\partial_X\left(\frac{f_0(X)}{\partial_X x}\right),\ X \in \Gamma^0,\ t > 0, \tag{3.17}$$

$$(\partial_X x)^{m-1}\partial_t x = -\frac{m}{m-1}\frac{\partial_X[f_0(X)^{m-1}]}{\partial_X x},\ X \in \partial\Gamma^0,\ t > 0, \tag{3.18}$$

$$x(X,0) = X,\ X \in \Gamma^0, \tag{3.19}$$

- Case 2.

$$\frac{(\partial_X x)^{m+1}}{m f_0(X)^m}\partial_t x = \partial_X\left(\frac{\partial_X x}{f_0(X)}\right),\ X \in \Gamma^0,\ t > 0, \tag{3.20}$$

$$(\partial_X x)^{m-1}\partial_t x = -\frac{m}{m-1}\frac{\partial_X[f_0(X)^{m-1}]}{\partial_X x},\ X \in \partial\Gamma^0,\ t > 0, \tag{3.21}$$

$$x(X,0) = X,\ X \in \Gamma^0. \tag{3.22}$$

Remark 3.3. Taking into account that $f_0(X) = 0$ at the boundary of its support, the boundary equation (3.18) and (3.21) is just the equation (3.17).

Let $h := (\xi_2^0 - \xi_1^0)/M$ be the spatial step. Then we partition the interval Γ^0 into equal subinterval with $X_i = \xi_1^0 + ih$, $0 \leq i \leq M$.

The **fully discrete** schemes read: Given the initial state $f_0(X)$ with a compact support Γ^0 and $\{x_i^n\}_{i=0}^M$, find $\{x_i^{n+1}\}_{i=0}^M$ such that

- Case 1.

$$\frac{f_0(X_i)}{m\left(\frac{f_0(X)}{D_h x^n}\right)_i^{m-1}} \cdot \frac{x_i^{n+1} - x_i^n}{\tau} = -d_h\left(\frac{f_0(X)}{D_h x^{n+1}}\right)_i,\ 0 < i < M, \tag{3.23}$$

$$(\bar{D}_h x_i^n)^{m-1} \cdot \frac{x_i^{n+1} - x_i^n}{\tau} = -\frac{m}{m-1} \cdot \frac{\bar{D}_h[f_0(X_i)^{m-1}]}{\bar{D}_h x_i^{n+1}},\ i = 0, M, \tag{3.24}$$

where

$$\bar{D}_h l_i := \begin{cases} \frac{l_{i+1}-l_i}{h}, & i = 0, \\ \frac{l_i - l_{i-1}}{h}, & i = M, \end{cases} \qquad \forall l = (l_0, \cdots, l_M). \tag{3.25}$$

- Case 2.

$$\frac{(\widetilde{D}_h x^n)_i^{m+1}}{m f_0(X_i)^m} \cdot \frac{x_i^{n+1} - x_i^n}{\tau} = d_h\left(\frac{D_h x^{n+1}}{f_0(X)}\right)_i,\ 1 \leq i \leq M-1, \tag{3.26}$$

$$(\bar{D}_h x_i^n)^{m-1} \cdot \frac{x_i^{n+1} - x_i^n}{\tau} = -\frac{m}{m-1} \cdot \frac{\bar{D}_h[f_0(X_i)^{m-1}]}{\bar{D}_h x_i^{n+1}},\ i = 0, M. \tag{3.27}$$

Comparing with the schemes (3.11) and (3.15), we have two more nonlinear equations at the boundary. The damped Newton's iteration shall be applied to solve the whole system.

Remark 3.4. Note that the equation (3.26) is linear but the boundary equation (3.27) is chosen to be nonlinear, the same as (3.24). If we choose a linear boundary equation as

$$(\bar{D}_h x_i^n)^{m+1} \cdot \frac{x_i^{n+1} - x_i^n}{\tau} = -\frac{m}{m-1} \cdot \bar{D}_h[f_0(X_i)^{m-1}] \cdot \bar{D}_h x_i^{n+1},\ i = 0, M,$$

then the matrix of the whole linear system would not be a M-matrix and the conservation of positivity would be destroyed.

When the right side of equation (3.24) is zero, the waiting phenomenon occurs. During the waiting time, the boundary condition in (3.18) or (3.21) should be replaced by $x_t = 0, X \in \partial\Gamma^0$ and the boundary condition in (3.24) or (3.27) should be replaced by $x_0^{n+1} = \xi_1^0,\ x_M^{n+1} = \xi_2^0$. The key problem is how to predict when the waiting stops. For the details to treat this kind of problem, see the algorithm in Section 5, Example 3.

4. Analysis of the numerical schemes

In this section, we perform detailed analyses for the numerical schemes (3.11) and (3.15), including the unique solvability in admissible set, the optimal rate convergence analysis, the convergence of Newton's iteration and the dissipation analysis of the total energy.

A few more notations have to be introduced. Let $l,\ g \in \mathcal{E}_M$ and $\phi,\ \varphi \in \mathcal{C}_M$. We define the *inner product* on space $\mathcal{E}_M$ and $\mathcal{C}_M$ respectively as:

$$\langle l, g\rangle := h\left(\frac{1}{2} l_0 g_0 + \sum_{i=1}^{M-1} l_i g_i + \frac{1}{2} l_M g_M\right), \tag{4.1}$$

$$\langle \phi, \varphi\rangle_e := h \sum_{i=0}^{M-1} \phi_{i+\frac{1}{2}} \varphi_{i+\frac{1}{2}}. \tag{4.2}$$

The following summation by parts formula is available:

$$\langle l, d_h \phi\rangle = -\langle D_h l, \phi\rangle_e,\ \text{with } l_0 = l_M = 0, \phi \in \mathcal{C}_M, l \in \mathcal{E}_M. \tag{4.3}$$

The inverse inequality is available:

$$\|l\|_\infty \le C_m \frac{\|l\|_2}{h^{1/2}},\quad \forall l \in \mathcal{E}_M, \tag{4.4}$$

where

$$\|l\|_\infty := \max_{0\le i\le M}\{l_i\} \text{ and } \|l\|_2^2 := \langle l, l\rangle.$$

First we prove that there exists a unique solution in admissible set $\mathcal{Q}$.

Theorem 4.1. *Suppose $f_0(X) \in \mathcal{E}_M$ is the initial state with a positive lower bound for $X \in \mathcal{Q}$. The numerical scheme (3.11) is uniquely solvable in $\mathcal{Q}$, and the solution x^{n+1} to the linear scheme (3.15) also belongs to $\mathcal{Q}$, for $n = 1, \cdots, N-1$.*

Proof. To prove the existence and uniqueness of solution in $\mathcal{Q}$ to the scheme (3.11), we first consider the following optimization problem:

$$\min_{y\in\bar{\mathcal{Q}}} J(y) := \frac{1}{2\tau}\left\langle \frac{f_0(X)}{m\left(\frac{f_0(X)}{\bar{D}_h x^n}\right)^{m-1}}(y - x^n), (y - x^n)\right\rangle + \left\langle f_0(X), \ln\left(\frac{f_0(X)}{D_h y}\right)\right\rangle_e, \tag{4.5}$$

where $x^n \in \mathcal{Q}$ is the position of particles at time t^n, $n = 0, \cdots, N-1$. Since $J(y)$ is a convex function on the closed convex set $\bar{\mathcal{Q}}$, there exists a unique minimizer $x \in \bar{\mathcal{Q}}$. Moreover, we must have $x \in \mathcal{Q}$, since for $\forall\ y \in \partial\mathcal{Q}$, there exists some $i > 0$ such that $(D_h y)_{i-1/2} = (y_i - y_{i-1})/h = 0$, then $J(y) = +\infty$.

Next we want to prove that $x \in \mathcal{Q}$ is the minimizer of $J(y)$ if and only if it is a solution to scheme (3.11). Then we can claim that the fully discrete scheme (3.11) has a unique solution.

In fact, if $x \in \mathcal{Q}$ is the minimizer of $J(y)$, then for $\forall y \in \bar{\mathcal{Q}}$, there exists a sufficiently small $\varrho_0 > 0$, such that for any $\varrho \in (-\varrho_0, \varrho_0)$, $x + \varrho(y - x) \in \mathcal{Q}$ since $\mathcal{Q}$ is a open convex set. Then $j(\varrho) := J(x + \varrho(y - x))$ achieves its minimal at $\varrho = 0$. So we have $j'(0) = 0$ and using summation by parts, we obtain

$$\frac{1}{\tau}\left\langle \frac{f_0(X)}{m\left(\frac{f_0(X)}{\bar{D}_h x^n}\right)^{m-1}}(x - x^n), y - x\right\rangle + \left\langle d_h\left(\frac{f_0(X)}{D_h x^{n+1}}\right), y - x\right\rangle = 0,$$

for any $y \in \bar{\mathcal{Q}}$. This implies that $x \in \mathcal{Q}$ satisfies (3.11).

Conversely let $x \in \mathcal{Q}$ be the solution to scheme (3.11). We need to prove that x is the minimizer of $J(y)$ on $\bar{\mathcal{Q}}$.

For any $y \in \partial\mathcal{Q}$, we always have $J(y) \geq J(x)$ due to $J(y) = +\infty$. Then for any $y \in \mathcal{Q}$, taking the inner product of (3.11) with $y - x$ and using summation by parts, we have

$$\frac{1}{\tau}\Big\langle \frac{f_0(X)}{m\big(\frac{f_0(X)}{D_h x^n}\big)^{m-1}}(x - x^n), y - x\Big\rangle - \Big\langle \frac{f_0(X)}{D_h x}, D_h(y - x)\Big\rangle_e = 0. \tag{4.6}$$

After the direct calculation, we get for any $y \in \mathcal{Q}$ such that

$$\begin{aligned} J(y) = J(x + (y - x)) &= J(x) + \frac{1}{2\tau}\Big\langle \frac{f_0(X)}{m\big(\frac{f_0(X)}{D_h x^n}\big)^{m-1}}(y - x), y - x\Big\rangle \\ &\quad + \frac{1}{\tau}\Big\langle \frac{f_0(X)}{m\big(\frac{f_0(X)}{D_h x^n}\big)^{m-1}}(x - x^n), y - x\Big\rangle + \Big\langle f_0(X), \ln\Big(\frac{D_h x}{D_h y}\Big)\Big\rangle_e \\ &\geq J(x), \end{aligned} \tag{4.7}$$

where the last inequality is obtained from (4.6) and the fact: $\ln\frac{1}{z} \geq -(z-1)$, $\forall z \in \mathbb{R}^+$, which leads to

$$\Big\langle f_0(X), \ln\Big(\frac{D_h x}{D_h y}\Big)\Big\rangle_e \geq -\Big\langle f_0(X), \frac{D_h(y - x)}{D_h x}\Big\rangle_e.$$

Then we prove that the solution to the numerical scheme (3.15) $x^{n+1} \in \mathcal{Q}$ if given $x^n \in \mathcal{Q}$, $n = 0, \cdots, N-1$. Without loss of generality, let $\bar{\Omega} = [0, 1]$. Due to the boundary condition (2.13), we have

$$x_0^{n+1} = 0,\ x_M^{n+1} = 1.$$

Based on the discrete extremum principle, we obtain that

$$0 < x_i^{n+1} < 1,\ i = 1, \cdots, M-1,\ n = 0, \cdots, N-1. \tag{4.8}$$

Suppose $x^{n+1} \notin \mathcal{Q}$, i.e., $\exists\ k_1,\ k_2 \in \mathbb{N}^+$ such that $k_1 < k_2$ and

$$0 < x_{k_1-1}^{n+1} < x_{k_1}^{n+1} \geq x_{k_1+1}^{n+1} \geq \cdots \geq x_{k_2-1}^{n+1} \geq x_{k_2}^{n+1} < x_{k_2+1}^{n+1} < 1. \tag{4.9}$$

Checking the equation (3.15) at $i = k_1$ and $i = k_2$ respectively, we have

$$x_{k_1}^{n+1} < x_{k_1}^n < x_{k_2}^n < x_{k_2}^{n+1},$$

which contradicts with (4.9). Due to the initial state $X \in \mathcal{Q}$, then $x^n \in \mathcal{Q}$, $n = 0, \cdots, N$. The proof is finished. □

Next we prove that the numerical scheme (3.11) and (3.15) satisfy the corresponding discrete energy dissipation laws.

Theorem 4.2. *Suppose the initial state $f_0(X) \in \mathcal{E}_M$ is positive and bounded for $X \in \mathcal{Q}$.*

- *Case 1. Let $x^n = (x_0^n, ..., x_M^n) \in \mathcal{Q}$, $n = 0, 1, \cdots, N-1$, be the solution to scheme (3.11) at time t^n. Then the discrete energy dissipation law holds, i.e.,*

$$\frac{E_N^{(1)}(x^{n+1}) - E_N^{(1)}(x^n)}{\tau} \leq -\Big\langle \frac{f_0(X)}{m\big(\frac{f_0(X)}{D_h x^n}\big)^{m-1}}\frac{x^{n+1} - x^n}{\tau}, \frac{x^{n+1} - x^n}{\tau}\Big\rangle, \tag{4.10}$$

  where

$$E_N^{(1)}(x) := \Big\langle f_0(X), \ln\Big(\frac{f_0(X)}{D_h x}\Big)\Big\rangle_e,\ \ \textit{with}\ \frac{\delta E_N^{(1)}(x)}{\delta x} = d_h\Big(\frac{f_0(X)}{D_h x}\Big). \tag{4.11}$$

- *Case 2. Let $x^n = (x_0^n, ..., x_M^n) \in \mathcal{Q}$, $n = 0, 1, \cdots, N-1$, be the solution to scheme (3.15) at time t^n. Then the following discrete energy dissipation law holds, i.e.,*

$$\frac{E_N^{(2)}(x^{n+1}) - E_N^{(2)}(x^n)}{\tau} \leq -\Big\langle \frac{(\widetilde{D}_h x^n)^{m+1}}{m f_0(X)^m}\cdot\frac{x^{n+1} - x^n}{\tau}, \frac{x^{n+1} - x^n}{\tau}\Big\rangle, \tag{4.12}$$

  where

$$E_N^{(2)}(x) := \frac{1}{2}\Big\langle \frac{D_h x}{f_0(X)}, D_h x\Big\rangle_e,\ \ \textit{with}\ \frac{\delta E_N^{(2)}(x)}{\delta x} = -d_h\Big(\frac{D_h x}{f_0(X)}\Big). \tag{4.13}$$

Note that (4.10) and (4.12) are the discrete counterpart of energy laws (2.10) and (2.12).

Proof. In Case 1, thanks to the convexity of $E_N^{(1)}(x)$, we have

$$\frac{E_N^{(1)}(x^n) - E_N^{(1)}(x^{n+1})}{\tau} \geq \left\langle \frac{\delta E_N^{(1)}(x^{n+1})}{\delta x}, \frac{x^n - x^{n+1}}{\tau} \right\rangle = \left\langle d_h\left(\frac{f_0(X)}{D_h x^{n+1}}\right), \frac{x^n - x^{n+1}}{\tau} \right\rangle$$
$$= \left\langle \frac{f_0(X)}{m\left(\frac{f_0(X)}{D_h x^n}\right)^{m-1}} \frac{x^n - x^{n+1}}{\tau}, \frac{x^n - x^{n+1}}{\tau} \right\rangle.$$

That means (4.10) holds. Due to the convexity of $E_N^{(2)}(x)$, we can also prove that the numerical scheme (3.15) satisfies the discrete energy dissipation law (4.12) in the similar way. □

The optimal rate convergence result for the schemes (3.11) and (3.15) is stated below.

Theorem 4.3. *Assume that the initial function $f_0(X)$ is positive and bounded, i.e., $0 < b_f \leq f_0(X) \leq B_f$. Denote $x_e \in \Omega$ as the exact solution to the original trajectory equation (2.9) or (2.11) with enough regularity and $x_h \in \mathcal{Q}$ as the numerical solution to the numerical scheme (3.11) in Case 1 or (3.15) in Case 2. The numerical error function is defined at a point-wise level:*

$$e_i^n = x_{e_i}^n - x_{h_i}^n, \tag{4.14}$$

where $x_{e_i}^n,\ x_{h_i}^n \in \mathcal{Q}$, $0 \leq i \leq N$, $n = 0, \cdots, M$. Then

- $e^n = (e_0^n, \cdots, e_M^n)$ *satisfies*

$$\|e^n\|_2 := \langle e^n, e^n \rangle \leq C(\tau + h^2).$$

- $\widetilde{D}_h e^n = (\widetilde{D}_h e_0^n, \cdots, \widetilde{D}_h e_M^n)$ *satisfies*

$$\|\widetilde{D}_h e^n\|_2 \leq C(\tau + h^2).$$

Moreover, the error between the numerical solution f_h^n and the exact solution f_e^n of the problem (2.1)-(2.3) can be estimated by:

$$\|f_h^n - f_e^n\|_2 \leq C(\tau + h^2),$$

where C is a positive constant, h is the spatial step, τ is the time step and $n = 0, \cdots, N$.

The proof is based on a technique of higher order expansion [15,45]. The technical details are skipped for the sake of brevity.

The following result is on the convergence of damped Newton's iteration (3.12)-(3.13).

Theorem 4.4. *Suppose the initial data $f_0(X) \in \mathcal{E}_M$ is positive and bounded for $X \in \mathcal{Q}$, then Newton's iteration (3.12)-(3.13) is convergent in $\mathcal{Q}$.*

In more details, we can first prove that $J(y)$, defined in (4.5), is a self-concordant function [33,14]. Then based on Theorem 2.2.3 in [33], damped Newton's iteration (3.12)-(3.13) is convergent in $\mathcal{Q}$. We omit the details.

5. Numerical results

In this section, we show some numerical results. To demonstrate the accuracy of the numerical schemes, in the first example, we solve a problem with a smooth solution. In the second example, we consider a free boundary problem with a exact Barenblatt solution. We check the convergence for the solution and the finite speed of propagation. In the third example, we focus on numerical simulation for the waiting time. Finally we report some results for problems with two support sets at the initial state in Example 4.

The error of a numerical solution is measured in the $\mathcal{L}^2$ and $\mathcal{L}^\infty$ norms defined as:

$$\|e_h\|_2^2 = \frac{1}{2}\left(e_{h_0}^2 h_{x_0} + \sum_{i=1}^{M-1} e_{h_i}^2 h_{x_i} + e_{h_M}^2 h_{x_M}\right), \tag{5.1}$$

and

$$\|e_h\|_\infty = \max_{0 \leq i \leq M} \{|e_{h_i}|\}, \tag{5.2}$$

Table 1
Example 1. Convergence rate of solution f and trajectory x in Case 1 at final time $T = 0.05$.

$m = \frac{5}{3}$										
M	τ	$\mathcal{L}^2$-error (f)	Order	$\mathcal{L}^\infty$-error(f)	Order	$\mathcal{L}^2$-error (x)	Order	$\mathcal{L}^\infty$-error (x)	Order	CPU (s)
100	1/100	1.1304e-02		1.6847e-02		1.5122e-03		2.2356e-03		0.1872
200	1/400	2.6730e-03	2.1144	3.8606e-03	2.1820	3.5665e-04	2.1200	5.2869e-04	2.1143	0.6084
400	1/1600	6.4528e-04	2.0712	9.2707e-04	2.0821	8.6042e-05	2.0725	1.2761e-04	2.0716	2.1840
800	1/6400	1.5246e-04	2.1163	2.1878e-04	2.1187	2.0324e-05	2.1167	3.0145e-05	2.1165	8.7361
$m = 2$										
M	τ	$\mathcal{L}^2$-error (f)	Order	$\mathcal{L}^\infty$-error(f)	Order	$\mathcal{L}^2$-error (x)	Order	$\mathcal{L}^\infty$-error (x)	Order	CPU (s)
100	1/100	8.4443e-03		1.2463e-02		1.1269e-03		1.1269e-03		0.1716
200	1/400	1.8021e-03	2.3429	2.5826e-03	2.4129	2.3982e-04	2.3494	2.3982e-04	2.3494	0.5304
400	1/1600	4.1921e-04	2.1495	5.9831e-04	2.1583	5.5749e-05	2.1509	5.5749e-05	2.1509	2.0748
800	1/6400	9.8039e-05	2.1379	1.3980e-04	2.1399	1.3034e-05	2.1386	1.3034e-05	2.1386	8.0185

$\mathcal{L}^2$-error and $\mathcal{L}^\infty$-error is defined by (5.1) and (5.2), respectively.
τ is the time step and $h = \frac{1}{M}$ is the space step.
CPU (s) is the CPU time (seconds).

Table 2
Example 1. Convergence rate of solution f and trajectory x in Case 2 at final time $T = 0.05$.

$m = \frac{5}{3}$										
M	τ	$\mathcal{L}^2$-error (f)	Order	$\mathcal{L}^\infty$-error (f)	Order	$\mathcal{L}^2$-error (x)	Order	$\mathcal{L}^\infty$-error (x)	Order	CPU(s)
100	1/100	1.0617e-02		1.6396e-02		1.4212e-03		2.0955e-03		0.0000
200	1/400	2.5002e-03	2.1233	3.6535e-03	2.2439	3.3374e-04	2.1291	4.9444e-04	2.1190	0.0000
400	1/1600	6.0295e-04	2.0733	8.7321e-04	2.0920	8.0425e-05	2.0749	1.1922e-04	2.0736	1.5600e-02
800	1/6400	1.4238e-04	2.1174	2.0580e-04	2.1215	1.8987e-05	2.1179	2.8150e-05	2.1176	6.2400e-02
$m = 2$										
M	τ	$\mathcal{L}^2$-error (f)	Order	$\mathcal{L}^\infty$-error (f)	Order	$\mathcal{L}^2$-error (x)	Order	$\mathcal{L}^\infty$-error (x)	Order	CPU(s)
100	1/100	8.0516e-03		1.2168e-02		1.0750e-03		1.5887e-03		0.0000
200	1/400	1.7134e-03	2.3497	2.4675e-03	2.4656	2.2803e-04	2.3572	3.3833e-04	2.3479	0.0000
400	1/1600	3.9861e-04	2.1492	5.7051e-04	2.1625	5.3010e-05	2.1508	7.8690e-05	2.1498	1.5600e-02
800	1/6400	9.3216e-05	2.1381	1.3324e-04	2.1409	1.2392e-05	2.1388	1.8397e-05	2.1386	6.2400e-02

$\mathcal{L}^2$-error and $\mathcal{L}^\infty$-error is defined by (5.1) and (5.2), respectively.
τ is the time step and $h = \frac{1}{M}$ is the space step.
CPU (s) is the CPU time (seconds).

where $e_h = (e_{h_0}, e_{h_1}, \cdots, e_{h_M})$ and for the error of the density $f - f_h$,

$$h_{x_i} = x_{i+1} - x_{i-1}, \quad 1 \le i \le M-1; \quad h_{x_0} = x_1 - x_0; \quad h_{x_M} = x_M - x_{M-1},$$

and for the error of the trajectory $x - x_h$,

$$h_{x_i} = 2h, \quad 1 \le i \le M-1, \quad h_{x_0} = h_{x_M} = h,$$

where h is the spatial step.

Example 1 *(Convergence rate for problem with smooth solution).* Consider the problem (2.1)-(2.3) in dimension one with a smooth positive initial state

$$f_0(x) = \sin(\pi x) + 0.5, \quad x \in \Omega = (0, 1). \tag{5.3}$$

We solve the trajectory equation (2.9) in Case 1 ((2.11) in Case 2) with the initial and boundary condition (2.13)-(2.14) by the fully discrete scheme (3.11) in Case 1 ((3.15) in Case 2) and approximate the density function f in (2.5) by (3.16). The reference 'exact' solution is obtained numerically on a much fine mesh with $h = \frac{1}{100000}$, $\tau = \frac{1}{100000}$.

Tables 1 and 2 show the convergence rate in Cases 1 and 2, respectively. The rate for density f and trajectory x in the $\mathcal{L}^2$ and $\mathcal{L}^\infty$ norm is 2nd order in space and 1st order in time for each scheme. But the linear scheme (3.15) in Case 2 is more efficient.

Example 2 *(Numerical finite propagation speed for problem with free boundary).* Barenblatt solution [3,38,44,48] in dimension one can be expressed by

$$B_m(x,t) = (t+1)^{-k}\Big(1 - \frac{k(m-1)}{2m}\frac{|x|^2}{(t+1)^{2k}}\Big)_+^{1/(m-1)}, \ x \in \mathbb{R}, \ t \ge 0, \tag{5.4}$$

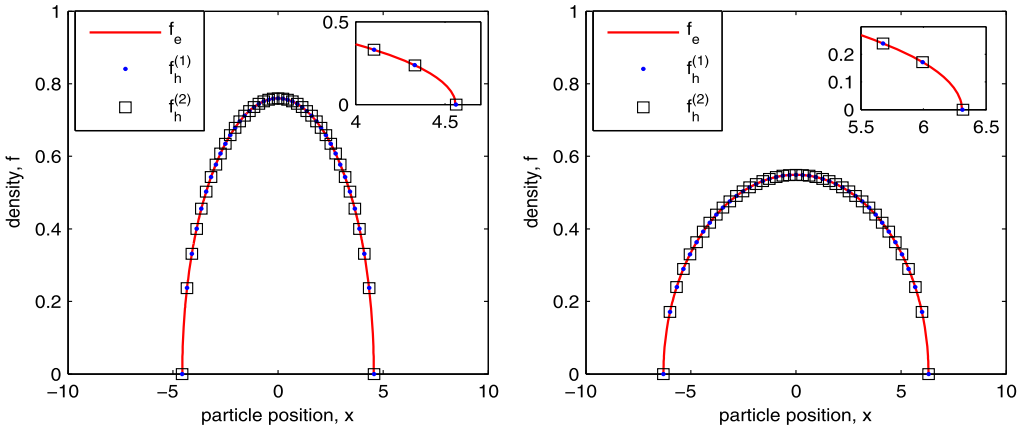

(a) $t = 2$ (b) $t = 10$

Fig. 1. Example 2. The evolution of f; f_e is the exact solution; $f_h^{(1)}$ and $f_h^{(2)}$ are numerical solutions in Case 1 and Case 2, respectively ($m = 3$, $M = 2000$, $\tau = 1/1000$).

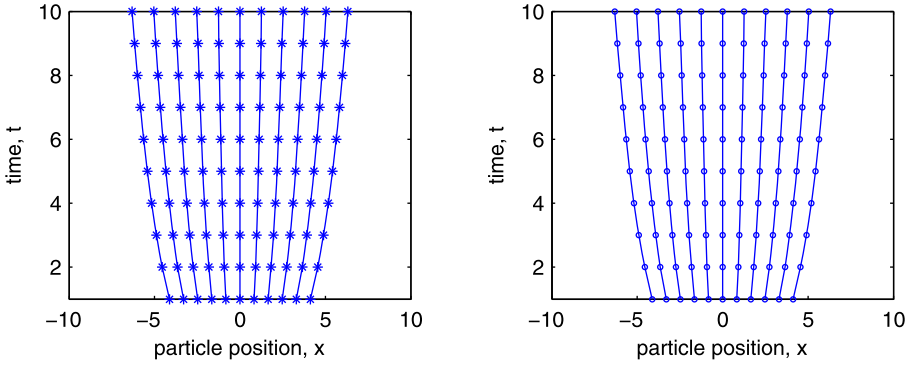

(a) The trajectory in Case 1 (b) The trajectory in Case 2

Fig. 2. Example 2. The evolution of particle position for $m = 3$ over time ($M = 2000$, $\tau = 1/1000$).

where $l_+ = \max\{l, 0\}$ and $k = (m+1)^{-1}$. The solution has a compact support $[-\xi_m^B(t), \xi_m^B(t)] \subsetneqq \Omega$ with the interface $|x| = \xi_m^B(t)$ moving outward in a finite speed, where

$$\xi_m^B(t) := \sqrt{\frac{2m}{k(m-1)}} \cdot (t+1)^k. \tag{5.5}$$

Let the computing domain be $\Omega = (-10, 10)$. We take Barenblatt profile $B_m(x, 0)$ as the initial data in problem (2.1)-(2.3). For a finite time interval, the interface can not reach the boundary of Ω, so the boundary condition (2.3) is valid. We solve the trajectory equation (3.17)-(3.19) in Case 1 ((3.20)-(3.22) in Case 2) by the fully discrete scheme (3.23)-(3.24) in Case 1 ((3.26)-(3.27) in Case 2).

Fig. 1 shows the numerical and exact solutions for $m = 3$ at time $t = 2$ and $t = 10$. The results demonstrate that the numerical solutions in Case 1 and Case 2 can approximate to the exact solution without oscillation. The evolution of the trajectory in both cases over time for $m = 3$ is shown in Fig. 2: particles move outward in a finite speed without twisting or exchanging. Fig. 3 shows the evolution of the right interface for numerical solutions and the exact solution with different m ($m = \frac{5}{3}$, $m = 3$) in Case 1 and Case 2. Table 3 shows the error of the right interface with different m ($m = \frac{5}{3}$, $m = 2$, $m = 3$, $m = 5$) at time $T = 1$. The results mean that the numerical interface in each case is a good approximation to the exact one and moves in a finite speed.

Table 4 shows the convergence rate of f in Case 1 and Case 2. We present the error in $\mathcal{L}^2$ norm and the error at $X = 0$ at time $T = 1$ for $m = 5/3$ and $m = 3$. The results show that the convergence rate is deteriorated when m is getting large since the regularity of the solution is getting lower and lower. The error of f at $X = 0$ keeps the rate of 2nd order since f is still smooth far away from the interface. Both numerical schemes have the same rate, but the error of f in Case 2 is larger. Table 5 shows the error of f in $\mathcal{L}^\infty$ norm for $m = \frac{5}{3}$. Both schemes are convergent in $\mathcal{L}^\infty$ norm at 1st order.

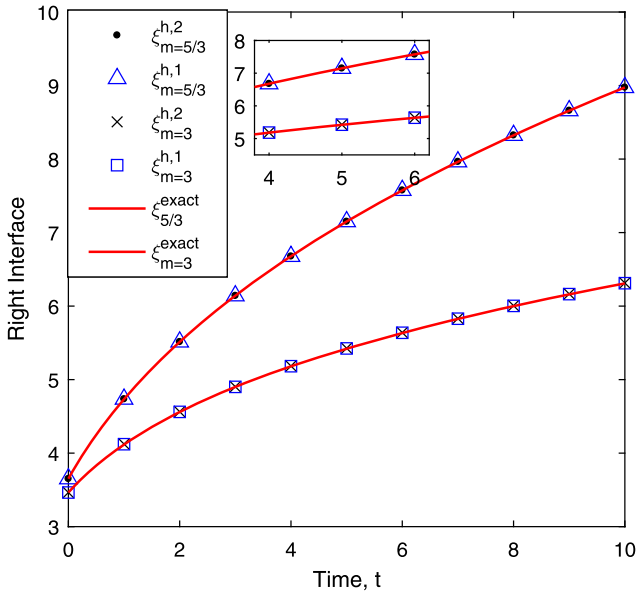

Fig. 3. Example 2. The evolution of the right interface over time for different m ($M = 2000$ and $\tau = 1/1000$); $\xi^{h,1}$ and $\xi^{h,2}$ denote the numerical interfaces in Case 1 and Case 2, respectively ($M = 2000$, $\tau = 1/1000$).

Table 3
Example 2. The error of right interface ξ_r at $T = 1$.

m	$\frac{5}{3}$	2	3	5
$\lvert\xi_r^{h,1} - \xi_r^{exact}\rvert$	6.6911e-04	2.3153e-04	2.9872e-03	5.1647e-03
$\lvert\xi_r^{h,2} - \xi_r^{exact}\rvert$	9.6066e-04	3.9205e-03	6.2808e-03	6.8532e-03

ξ_r^{exact} denotes the exact right interface; $\xi_r^{h,1}$ and $\xi_r^{h,2}$ denote the numerical right interfaces in Case 1 and Case 2, respectively.

Table 4
Example 2. The convergence rate of f at the finite time $T = 1$.

$m = \frac{5}{3}$									
M	τ	$\mathcal{L}^2$-error $(f_h^{(1)})$	Order	$\mathcal{L}^2$-error $(f_h^{(2)})$	Order	Error at $X=0$ $(f_h^{(1)})$	Order	Error at $X=0$ $(f_h^{(2)})$	Order
1000	1/250	5.6454e-05		6.1225e-04		2.5417e-05		2.7701e-04	
2000	1/1000	1.4133e-05	1.9972	1.5281e-04	2.0033	6.3626e-06	1.9974	6.9154e-05	2.0029
4000	1/4000	3.5351e-06	1.9990	3.8184e-05	2.0009	1.5912e-06	1.9993	1.7282e-05	2.0007
8000	1/16000	8.8404e-07	1.9994	9.5445e-06	2.0003	3.9782e-07	1.9998	4.3202e-06	2.0002
$m = 3$									
M	τ	$\mathcal{L}^2$-error $(f_h^{(1)})$	Order	$\mathcal{L}^2$-error $(f_h^{(2)})$	Order	Error at $X=0$ $(f_h^{(1)})$	Order	Error at $X=0$ $(f_h^{(2)})$	Order
1000	1/250	1.3480e-03		5.8979e-03		4.1682e-05		1.9361e-04	
2000	1/1000	6.7614e-04	0.9969	2.4952e-03	1.1819	1.0821e-05	1.9259	4.9069e-05	1.9728
4000	1/4000	3.4194e-04	0.9887	1.2050e-03	1.0353	2.8617e-06	1.8907	1.2570e-05	1.9519
8000	1/16000	1.7310e-04	0.9877	6.0168e-04	1.0014	7.7215e-07	1.8531	3.2253e-06	1.9306

$f_h^{(1)}$ and $f_h^{(2)}$ are the numerical solutions of the problem (2.1)-(2.3) in Case 1 and Case 2, respectively.
$\mathcal{L}^2$-error $(f_h^{(i)})$ is the error of $f_h^{(i)}$ in $\mathcal{L}^2$ norm defined by (5.1), $i = 1, 2$.
τ is the time step; $h = \frac{1}{M}$ is the space step.

Example 3 *(Numerical simulation for the waiting time).* The waiting-time phenomenon occurs for a certain type of initial states [44]. Without loss of generality we consider the left interface. Similar argument can be obtained for the right interface. Recalling the trajectory equation (3.18) or (3.21) at the left interface, we have

$$\partial_t x = -\frac{m}{m-1}\frac{\partial_X[f_0(X)^{m-1}]}{(\partial_X x)^m}, \text{ at } X = \xi_1^0,\ t > 0, \tag{5.6}$$

where $f_0(X)$ is the smooth initial state with compact support $[\xi_1^0, \xi_2^0]$. At the initial time, $\partial_X x \equiv 1$, so if $\partial_X[f_0(X)^{m-1}] = 0$ at $X = \xi_1^0$, then $x_t(\xi_1^0, 0) = 0$ and it is possible to have a positive waiting time.

Table 5
Example 2. The convergent rate of f in $\mathcal{L}^\infty$ norm at final time $T=1$.

$m=\frac{5}{3}$					
M	τ	$\mathcal{L}^\infty$-error $(f_h^{(1)})$	Order	$\mathcal{L}^\infty$-error $(f_h^{(2)})$	Order
100	1/10	1.00e-03		7.46e-03	
250	1/25	2.65e-04	1.45	2.83e-03	1.06
1000	1/100	6.28e-05	1.04	6.93e-04	1.01
2500	1/250	2.51e-05	1.00	2.76e-04	1.00

$f_h^{(1)}$ and $f_h^{(2)}$ are the numerical solutions in Case 1 and Case 2, respectively.
$\mathcal{L}^\infty$-error (f_i), $i=1,2$ are the error of solution f in $\mathcal{L}^\infty$ norm defined by (5.2).

If the left interface keeps waiting till time $t^*>0$, then $\xi_1^t\equiv\xi_1^0$, for $t\le t^*$. This means that we must have, at $X=\xi_1^0$, $\partial_t x\equiv 0$, for $t<t^*$ and $\partial_t x<0$, for $t=t^*+\epsilon$ with any sufficiently small $\epsilon>0$. Hence the waiting time can be characterized as:

$$t^*:=\inf\left\{t>0: x_t=-\frac{m}{m-1}\frac{\partial_X[f_0(X)^{m-1}]}{(\partial_X x)^m}<0,\ \text{as } X\to\xi_1^0\right\}. \tag{5.7}$$

Noting that, at $X=\xi_1^0$, the numerator $\partial_X[f_0(X)^{m-1}]$ is fixed and only the denominator $(\partial_X x)^m$ changes when time evolves. If there exists a positive waiting time $t^*>0$, we must have that, at $X=\xi_1^0$, $\partial_X[f_0(X)^{m-1}]=0$ and as time evolves, $(\partial_X x)^m$ becomes smaller and smaller and comes to the same order infinitesimal as $\partial_X[f_0(X)^{m-1}]$ as $X\to\xi_1^0$ at time $t=t^*$. So we have another criterion for the waiting time:

$$t^* \text{ is the first time instant when } \mathcal{B}(t):=\frac{\partial_X[f_0(X)^{m-1}]}{(\partial_X x)^m}\nrightarrow 0,\ \text{as } X\to\xi_1^0. \tag{5.8}$$

Next we focus on finding the criterion for the numerical waiting time t_h^*. Let

$$\mathcal{B}_h^n:=\frac{\bar{D}_h[(f_0(X_0))^{m-1}]}{(\bar{D}_h x_{h,0}^n)^m},$$

where the difference operator $\bar{D}_h$ is defined in (3.25) and $x_h^n=(x_{h,0}^n,\cdots,x_{h,M}^n)$ is the numerical trajectory position at time t^n, $n=0,\cdots,N$.

The numerical waiting time t_h^* is determined by the following criterion:

$$t_h^*:=\min\left\{t^n:\left|\frac{\mathcal{B}_{2h}^n}{\mathcal{B}_h^n}\right|\le 1\right\}. \tag{5.9}$$

To get $\mathcal{B}_{2h}^n$ in the above formula, we need to know the trajectory x_{2h}^n. However, we don't need to solve the trajectory problem again by spacial step $2h$. We just select it from the given solution x_h^n, i.e., $x_{2h}^n=(x_{h,0}^n,x_{h,2}^n,x_{h,4}^n,\cdots,)$.

Remark 5.1. The numerical criterion (5.9) is an approximation of the continuous criterion (5.8) in the sense that if $\mathcal{B}(t)$ is infinitesimal as $X\to\xi_1^0$, then $\mathcal{B}_h<\mathcal{B}_{2h}$ for any sufficiently small $h>0$.

Now we present the algorithm for problems with waiting time.

Algorithm for Waiting time:

- **Step 1.** For time $t^n, n=0,1,\cdots$, solve the trajectory equation (3.17)-(3.19) in Case 1 ((3.20)-(3.22) in Case 2) by the fully discrete scheme (3.23)-(3.24) in Case 1 ((3.26)-(3.27) in Case 2) but replacing the boundary condition (3.18) in Case 1 ((3.21) in Case 2) by $\partial_t x=0$ and replacing the boundary condition (3.24) in Case 1 ((3.27) in Case 2) by $x_0^{n+1}=\xi_1^0,\ x_M^{n+1}=\xi_2^0$.
  Check the criterion (5.9) for x^{n+1}. If it is not valid, goto next time step. If it is valid, then set $t_h^*=t^{n+1}$. $n^*=n+1$ and goto Step 2.
- **Step 2.** For time $t^n, n=n^*,n^*+1,\cdots$, solve the trajectory equation (3.17)-(3.19) in Case 1 ((3.20)-(3.22) in Case 2) by the fully discrete scheme (3.23)-(3.24) in Case 1 ((3.26)-(3.27) in Case 2).

Remark 5.2. In the above algorithm, we introduce a manual switch between a numerical method for fixed support and a method with expansion. Notice that the original problem has a universal condition (5.6) at the boundary of the support no matter whether the interface is waiting there or moves at a finite speed. Why do we not discretize it directly as we have done in Section 3.3? During the waiting period, the right hand side of (5.6) is always zero. If we discretize (5.6) directly by

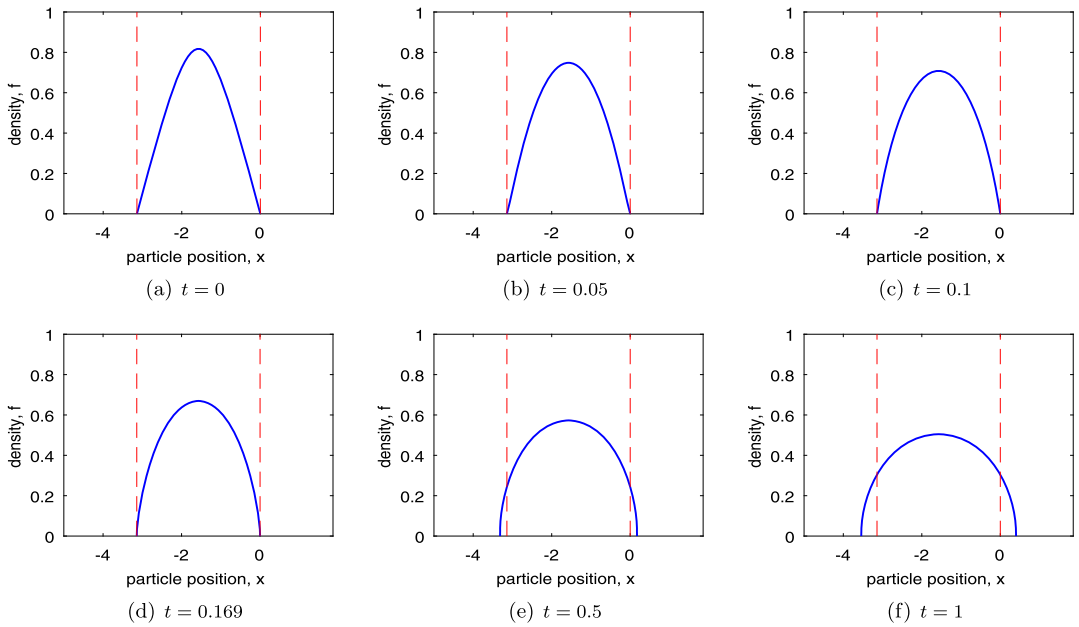

Fig. 4. Example 3. Waiting time: Evolution of solution f in Case 1 ($m = 3$, $M = 1000$, $\tau = 1/2000$).

some finite difference methods, it is inevitable to introduce an error, which means that the particles at boundary have an artificial speed now, though it may be small. Then it is not expectable to predict a correct waiting time. That is also the main reason why most existing works can not yield a right waiting time. Our approach is a reasonable numerical implementation of the boundary condition (5.6) when waiting phenomena occurs.

Now we consider the following data set-up:

$$\Omega = (-5, 5), \tag{5.10}$$

$$f_0(x) = \begin{cases} \left\{\frac{m-1}{m}[(1-\theta)\sin^2(x) + \theta\sin^4(x)]\right\}^{1/(m-1)}, & x \in [-\pi, 0], \\ 0, & \text{otherwise in } \Omega, \end{cases} \tag{5.11}$$

where $\theta \in [0, \frac{1}{4}]$. Then the waiting time is positive and the exact one [2] is:

$$t^*_{exact} = \frac{1}{2(m+1)(1-\theta)}. \tag{5.12}$$

Fig. 4 depicts that the evolution of numerical solution f over grid with spatial step $h = \pi/M$ ($M = 1000$) and the time step $\tau = 1/2000$ for $m = 3$ and $\theta = \frac{1}{4}$ in Case 1. The results show that the waiting time does exist. After the time about 0.169, the interface moves outward in a finite speed. In the whole process, we obtain the numerical solution without oscillation. Fig. 5 (a) and (b) present the comparison of the numerical and exact waiting time for different θ and m in Case 1 and Case 2. The results show that the numerical waiting time is a good approximation to the exact one in each case. Furthermore, Table 6 presents the error of waiting time for $m = 3$ and $\theta = \frac{1}{4}$ over different grids ($M = 500$, $\tau = 1/1000$; $M = 1000$, $\tau = 1/2000$; $M = 2000$, $\tau = 1/4000$; $M = 4000$, $\tau = 1/8000$) in Case 1 and Case 2. It shows that the numerical waiting time is convergent to the exact one in each case.

Example 4 *(Numerical simulation for problem with two separate support sets at initial time).* We now consider a problem with a step function as the initial state. In problem (2.1)-(2.3), let $m = 5$, $\Omega = (-5, 5)$ and

$$f_0(x) = \begin{cases} 1, & x \in (0.5, 3), \\ 1.5, & x \in (-3, -0.5), \\ 0, & \text{otherwise.} \end{cases} \tag{5.13}$$

The example models the movement and interaction of two supports. Before the two supports meet, we solve two problems independently. When the two supports meet at time t^*_m, we should reconstruct the two parts of solution into a whole

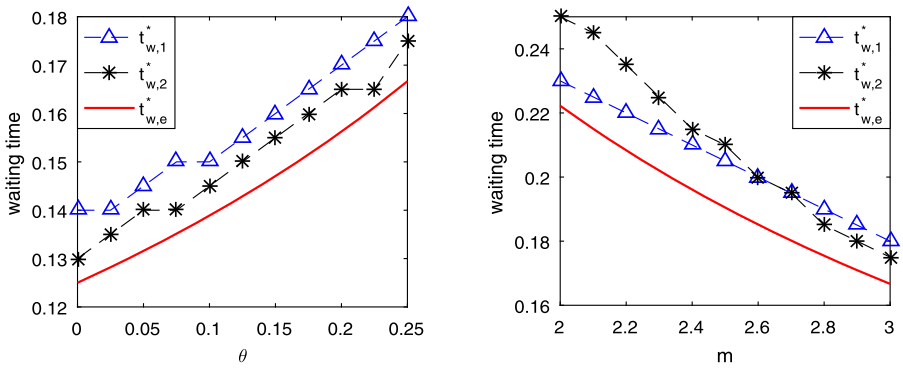

(a) the influence of θ ($m = 3$) (b) the influence of m ($\theta = \frac{1}{4}$)

Fig. 5. Example 3. Waiting time: the influence of θ and m; t_e^* is the exact waiting time given by (5.12); $t_{w,1}^*$ and $t_{w,2}^*$ are the numerical waiting time in Case 1 and Case 2, respectively ($M = 200$, $\tau = 1/200$).

Table 6
Example 3. The convergence rate of waiting time ($m = 3$, $\theta = \frac{1}{4}$).

M	τ	$t_{w,1}^*$	$\lvert t_{w,1}^* - t_{w,e}^*\rvert$	Order	CPU^1(s)	$t_{w,2}^*$	$\lvert t_{w,2}^* - t_{w,e}^*\rvert$	Order	CPU^2(s)
25	$\frac{1}{25}$	0.24	0.0733		4.6875e-02	0.24	0.0733		1.5625e-02
50	1/50	0.20	0.0333	1.1006	4.6875e-02	0.20	0.0333	1.1006	3.1250e-02
100	1/100	0.19	0.0233	0.7146	7.8125e-02	0.18	0.0133	1.2519	3.1250e-02
200	1/200	0.180	0.0133	0.8759	1.4063e-01	0.175	0.0083	0.8012	4.6875e-02
$t_{w,e}^*$		0.16667			0.16667				

$t_{w,e}^*$ is the exact waiting time by (5.12); $t_{w,1}^*$ and $t_{w,2}^*$ are the waiting time in Case 1 and 2, respectively.
CPU^1(s) and CPU^2(s) denote the CPU time (seconds) in Case 1 and 2, respectively.

with single support over an equidistance mesh and then take it as initial state to solve problem (3.17)-(3.19) in Case 1 ((3.20)-(3.22) in Case 2) starting from $t = t_m^*$.

The spatial step is chosen as $h = (3 - 0.5)/M$ ($M = 5000$) for each support and the time step is $\tau = 1/10000$. In Case 1, Figs. 6 (a)∼(c) show that as time evolves, the two supports expand and meet at time $t_m^* = 0.1415$. At this time, a reconstruction is taken by monotone piecewise cubic interpolation [18] over an equidistance grid with partition number $M_2 = 10000$, shown in Fig. 6(d). Figs. 6(e)∼(g) show the evolution after meeting. Oscillations do not appear around the free boundary during the whole process. Fig. 6(h) shows the movement of particles in this process. The numerical solution in Case 2 has the similar results and the meeting time is $t_m^* = 0.1383$.

Remark 5.3. The meeting time of two supports is defined as:

$$t_m^* := \inf_{t>0}\{|x_M^l - x_0^r| \le 10^{-10}\}, \tag{5.14}$$

where x_M^l is the endpoint of the left support and x_0^r the first point of right support.

6. Concluding remarks

In this paper, two numerical methods for PME based on EnVarA has been proposed and analyzed. Based on the total energy density $f \ln f$, the proposed numerical scheme is proven to be uniquely solvable on an admissible convex set. Based on the total energy density $\frac{1}{2f}$, the numerical scheme is linear. In turn, the energy dissipation rate of both schemes has been an outcome of the variational approach. According to the numerical simulation results for both schemes, no oscillation appears around the free boundary, and the finite propagation speed could be numerically calculated. We also give a criterion that can compute the waiting time and numerical convergence of the waiting time is reported, which is the first such result for this problem.

One obvious limitation of this work is associated with the one-dimensional nature of the problem. In two or higher dimension, the determinant of the deformation gradient, i.e., $\det \frac{\partial x}{\partial X}$, will arise in the trajectory equations, which is a fully nonlinear degenerate parabolic system. We have not found an efficient numerical method which can satisfy the discrete energy dissipation law. A similar numerical method, based on evolving diffeomorphisms [6], may also encounter the same problem. Solving for multi-dimensional PME by this energetic method will be left to our future works.

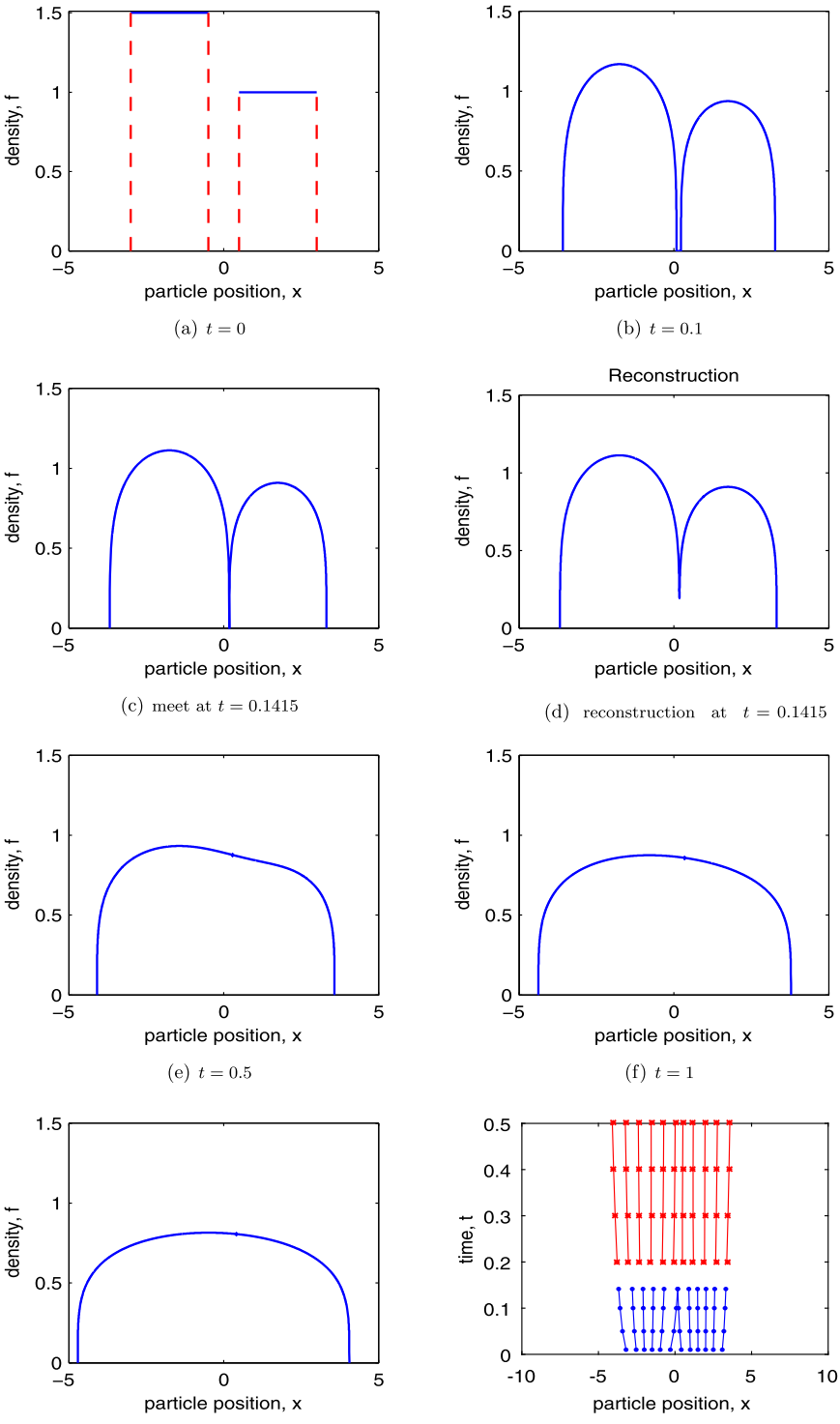

(a) $t = 0$ (b) $t = 0.1$

(c) meet at $t = 0.1415$ (d) reconstruction at $t = 0.1415$

(e) $t = 0.5$ (f) $t = 1$

(g) $t = 2$ (h) particle position

Fig. 6. Example 4. The evolution of density f and particle position x in Case 1 for $m = 5$ over time ($M = 5000$, $\tau = 1/10000$ and the space grid size of reconstruction $M_2 = 10000$).

Acknowledgements

This work is supported in part by NSF of China under the grants 11271281. Chun Liu and Cheng Wang are partially supported by NSF grants DMS-1216938, DMS-1418689, respectively.

References

[1] D.G. Aronson, Regularity properties of flows through porous media, SIAM J. Appl. Math. 17 (1969) 461–467.
[2] D.G. Aronson, L.A. Caffarelli, S. Kamin, How an initially stationary interface begins to move in porous medium flow, SIAM J. Math. Anal. 14 (4) (1983) 639–658.
[3] G.I. Barenblatt, On some unsteady motions of a liquid or a gas in a porous medium, Prikl. Mat. Meh. 16 (1) (1952) 67–78 (in Russian).
[4] M. Bertsch, R. Dal Passo, A numerical treatment of a super degenerate equation with applications to the porous media equation, Q. Appl. Math. 48 (1990) 133–152.
[5] J.A. Carrillo, J.S. Moll, Numerical simulation of diffusive and aggregation phenomena in nonlinear continuity equations by evolving diffeomorphisms, SIAM J. Sci. Comput. 31 (6) (2009) 4305–4329.
[6] J.A. Carrillo, H. Ranetbauer, M.T. Wolfram, Numerical simulation of nonlinear continuity equations by evolving diffeomorphisms, J. Comput. Phys. 327 (2016) 186–202.
[7] G. Chen, T. Huang, C. Liu, Finite time singularities for hyperbolic systems, SIAM J. Math. Anal. 47 (1) (2015) 758–785.
[8] W. Chen, S. Conde, C. Wang, X. Wang, S.M. Wise, A linear energy stable scheme for a thin film model without slope selection, J. Sci. Comput. 52 (3) (2012) 546–562.
[9] W. Chen, Y. Liu, X. Wang, S.M. Wise, Convergence analysis of a fully discrete finite difference scheme for Cahn-Hilliard-Hele-Shaw equation, Math. Comput. 85 (301) (2016) 2231–2257.
[10] K. Cheng, W. Feng, C. Wang, S.M. Wise, An energy stable fourth order finite difference scheme for the Cahn-Hilliard equation, J. Comput. Appl. Math. (2018), https://doi.org/10.1016/j.cam.2018.05.039, in press, published online.
[11] K. Cheng, C. Wang, S.M. Wise, X. Yue, A second-order, weakly energy-stable pseudo-spectral scheme for the Cahn-Hilliard equation and its solution by the homogeneous linear iteration method, J. Sci. Comput. 69 (3) (2016) 1083–1114.
[12] E. DiBenedetto, D. Hoff, An interface tracking algorithm for the porous medium equation, Trans. Am. Math. Soc. 284 (1984) 463–500.
[13] Q. Du, C. Liu, R. Ryham, X. Wang, Energetic variational approaches in modeling vesicle and fluid interactions, Physica D 238 (2009) 923–930.
[14] C. Duan, C. Liu, C. Wang, X. Yue, Numerical complete solution for random genetic drift by Energetic Variational approach, arXiv:1803.09436, 2018, Math. Model. Numer. Anal. (2019), https://doi.org/10.1051/m2an/2018058, in press, published online.
[15] W. E, J.G. Liu, Projection method I: convergence and numerical boundary layers, SIAM J. Numer. Anal. 32 (1995) 1017–1057.
[16] B. Eisenberg, Y.K. Hyon, C. Liu, Energy variational analysis of ions in water and channels: field theory for primitive models of complex ionic fluids, J. Chem. Phys. 133 (10) (2010) 104.
[17] D.J. Eyre, Unconditionally gradient stable time marching the Cahn-Hilliard equation, MRS Proc. 529 (1998) 39.
[18] F.N. Fritsch, R.E. Carlson, Monotone piecewise cubic interpolation, SIAM J. Numer. Anal. 17 (1980) 238–246.
[19] J.L. Graveleau, P. Jamet, A finite difference approach to some degenerate nonlinear parabolic equations, SIAM J. Appl. Math. 20 (1971) 199–223.
[20] J. Gratton, C. Vigo, Evolution of self-similarity, and other properties of waiting-time solutions of the porous medium equation: the case of viscous gravity currents, J. Appl. Math. 9 (1998) 327–350.
[21] J. Guo, C. Wang, S.M. Wise, X. Yue, An H^2 convergence of a second-order convex-splitting, finite difference scheme for the three-dimensional Cahn-Hilliard equation, Commun. Math. Sci. 14 (2) (2016) 489–515.
[22] Y. Hyon, D.Y. Kwak, C. Liu, Energetic variational approach in complex fluids: maximum dissipation principle, Discrete Contin. Dyn. Syst. 26 (4) (2010) 1291–1304.
[23] Z. Hu, S.M. Wise, C. Wang, J. Lowengrub, Stable and efficient finite-difference nonlinear-multigrid schemes for the phase field crystal equation, J. Comput. Phys. 228 (15) (2009) 5323–5339.
[24] S. Jin, L. Pareschi, G. Toscani, Diffusive relaxation schemes for multi-scale discrete-velocity kinetic equations, SIAM J. Numer. Anal. 35 (6) (1998) 2405–2439.
[25] A.S. Kalašnikov, Formation of singularities in solutions of the equation of nonstationary filtration, Ž. Vyčisl. Mat. Mat. Fiz. 7 (1967) 440–444.
[26] H. Koba, C. Liu, Y. Giga, Energetic variational approaches for incompressible fluid systems on an evolving surface, Q. Appl. Math. 75 (2017) 359–389.
[27] L.S. Leibenzon, The motion of a gas in a porous medium, in: Complete Works, vol. 2, Acad. Sciences URSS, Moscow, 1953 (in Russian).
[28] W. Li, W. Chen, C. Wang, Y. Yan, R. He, A second order energy stable linear scheme for a thin film model without slope selection, J. Sci. Comput. 76 (3) (2018) 1905–1937.
[29] C. Liu, J. Shen, A phase field model for the mixture of two incompressible fluids and its approximation by a Fourier-spectral method, Physica D 179 (3–4) (2003) 211–228.
[30] C. Liu, H. Wu, An energetic variational approach for the Cahn-Hilliard equation with dynamic boundary conditions, arXiv preprint, arXiv:1710.08318, 2017.
[31] M. Mimura, T. Nakaki, K. Tomoeda, A numerical approach to interface curves for some nonlinear diffusion equations, Jpn. J. Appl. Math. 1 (1984) 93–139.
[32] T. Nakaki, K. Tomoeda, Numerical approach to the waiting time for the one-dimensional porous medium equation, Q. Appl. Math. 61 (4) (2002) 601–612.
[33] Y. Nesterov, A. Nemirovskii, Interior-Point Polynomial Algorithms in Convex Programming, SIAM, 1994.
[34] C. Ngo, W.Z. Huang, A study on moving mesh finite element solution of the porous medium equation, J. Comput. Phys. 331 (2017) 357–380.
[35] O.A. Oleĭnik, A.S. Kalašinkov, Y. Čžou, The Cauchy problem and boundary problems for equations of the type of non-stationary filtration, Izv. Akad. Nauk SSSR, Ser. Mat. 22 (1958) 667–704.
[36] L. Onsager, Reciprocal relations in irreversible processes. II, Phys. Rev. 38 (1931) 2265–2279.
[37] L. Onsager, Reciprocal relations in irreversible processes. I, Phys. Rev. 37 (4) (1931) 405.
[38] R.E. Pattle, Diffusion from an instantaneous point source with concentration dependent coefficient, Q. J. Mech. Appl. Math. 12 (1959) 407–409.
[39] J. Shen, C. Wang, X. Wang, S.M. Wise, Second-order convex splitting schemes for gradient flows with Ehrlich-Schwoebel type energy: application to thin film epitaxy, SIAM J. Numer. Anal. 50 (1) (2012) 105–125.
[40] S.I. Shmarev, Interfaces in multidimensional diffusion equations with absorption terms, Nonlinear Anal. 53 (2003) 791–828.
[41] S. Shmarev, Interfaces in solutions of diffusion-absorption equations in arbitrary space dimension, in: Trends in Partial Differential Equations of Mathematical Physics, in: Prog. Nonlinear Differ. Equ. Appl., Birkhäuser, Basel, 2005, pp. 257–273.
[42] J.W. Strutt, Some general theorems relating to vibrations, Proc. Lond. Math. Soc. IV (1873) 357–368.
[43] K. Tomoeda, M. Mimura, Numerical approximations to interface curves for a porous medium equation, Hiroshima Math. J. 13 (1983) 273–294.
[44] J.L. Vázquez, The Porous Medium Equation, Oxford University Press, Oxford, 2007.
[45] C. Wang, J.G. Liu, Convergence of gauge method for incompressible flow, Math. Comput. 69 (2000) 1385–1407.
[46] C. Wang, S.M. Wise, An energy stable and convergent finite-difference scheme for the modified phase field crystal equation, SIAM J. Numer. Anal. 49 (3) (2011) 945–963.

[47] M. Westdickenberg, J. Wilkening, Variational particle schemes for the porous medium equation and for the system of isentropic Euler equations, ESAIM: M2AN 44 (1) (2010) 133–166.
[48] Ya.B. Zel'dovich, A.S. Kompaneets, Towards a theory of heat conduction with thermal conductivity depending on the temperature, in: Collection of Papers Dedicated to 70th Anniversary of A.F. Ioffe, Izd. Akad. Nauk SSSR, Moscow, 1950, pp. 61–72.
[49] Q. Zhang, Z.L. Wu, Numerical simulation for porous medium equation by local discontinuous Galerkin finite element method, J. Sci. Comput. 38 (2) (2009) 127–148.